Geologic map of the Batamote Hills 7½' Quadrangle, Pima County, Arizona

by:

Charles A. Ferguson, Bradford J. Johnson, and Todd C. Shipman

Arizona Geological Survey Digital Geologic Map DGM-32

November 2003

Scale 1:24,000 (1 sheet)

Arizona Geological Survey
416 W. Congress St., #100, Tucson, Arizona 85701

Research supported by the U.S. Geological Survey, National Cooperative Geologic Mapping Program, under USGS award number #02HQAG0016. The views and conclusions contained in this document are those of the authors and should not be interpreted as necessarily representing the official policies, either expressed or implied, of the U.S. Government.

Introduction

The Sierrita Mountains are a deeply eroded, ~1,000km^2 Basin and Range uplift located 60km south of Tucson, southern Arizona, USA. The Sierritas are dominated by a 35km diameter, 600m-high bajada surface that slopes up and terminates abruptly against a 300m-high, rugged, inselberg core range (~200km^2). The bajada is developed on a bedrock surface dominated by two rock types; Paleocene Ruby Star granodiorite (Tgd) in the north, and Cenozoic volcaniclastic conglomerate (Tcv) in the south. Low ranges of rugged hills, composed of Mid-Tertiary lava fields in the south, and strongly mineralized pre-Paleocene rocks in the north protrude through the bajada. The Batamote Hills quadrangle includes the southern half of the core range, and a large area of the southern piedmont.

Cenozoic geology

The southern piedmont of the Sierrita Mountains is underlain by a south-tilted (fanning upwards from 30^o to 0^o) Cenozoic volcaniclastic conglomerate sequence (Tcv). Older Pleistocene deposits are notably absent on the piedmont. Late Pleistocene deposits show evidence of strath terraces on Tcv forming during a period of equilibrium with respect to relative base-level. Interleaved within the conglomerate are two discrete Cenozoic lava fields, the Batamote Hills field to the west and the Tinaja Peak field to the east. Lavas in the two fields range from basalt to dacite in composition (Table 1, Figure 1) and each field is dominated by a young, phenocryst-rich dacite lava unit. Consistent, although subtle, differences in phenocryst mineralogy and geochemistry indicate that the dacites are different. Stratigraphic sequencing and composition of the other lavas are also distinctly different in each fields.

Southward tilting and the San Xavier fault

The map pattern of intrusive relationships at the Sierrita-Esperanza mine has been interpreted as the result of 40^o to 60^o of south-southeast tilting of the entire intrusive complex (Seedorff, 1983). Tilting of this magnitude is also supported by regional, consistently south-southeast tilts of the youngest Mesozoic volcanic rocks found throughout the range, the tilt of the basal Cenozoic unconformity, and the presence of the San Xavier fault, interpreted as a tilted low-angle normal fault located to the north of the map area. P. Jensen's (1998) argument that the complex has not been tilted significantly, and that tilting of the host rocks was caused by emplacement of plutonic rocks, does not account for the consistent orientation of southerly tilts well to the west and southwest of the intrusive zone(s).

The San Xavier fault, originally interpreted as a thrust (Cooper, 1973; L. Jansen, 1982), is shown schematically on our cross-sections as a low-angle normal fault with approximately 9km of top-to-the-north displacement. This displacement is based on the interpretation that the Mission mine, in its hanging wall, correlates with the Twin Buttes mine in its footwall (Cooper, 1960; Titley, 1982; L. Jansen, 1982: Williamson and Poulton, 1995). The position of the fault, shown in the "sky" on our cross-sections, is based on extrapolating structure contours of the fault surface (L. Jansen's Figure 22.1, 1982) to the west. The position of an Oligocene sequence of conglomerate, avalanche breccia and a distinctive plagioclase-porphyritic, coarse-grained andesite lava that dips to the south 50-70^o in the hanging wall is projected into our cross-sections. This sequence,

called the Helmet Conglomerate (Th) represents the initial stages of sedimentation in the hanging wall of the San Xavier detachment fault. A hypothetical reconstruction, shown in cross-section A-A'', shows the position of the base of the Helmet Conglomerate as it would have appeared in the footwall. This position is based primarily on L. Jansen's (1982) estimate of 9km of displacement on the fault. The Cenozoic conglomerate of the Batamote Hills quadrangle (Tcv), with significantly lower southerly dips, is shown hypothetically truncating and overlapping the San Xavier fault, and represents the waning stages of extension and sedimentation in the area.

Paleocene magmatism and porphyry copper mineralization

The northern third of the Batamote Hills quadrangle is underlain by strongly altered Mesozoic volcanic rocks intruded by a major Mesozoic pluton, the Mesozoic (177Ma) Harris Ranch Monzonite, actually a quartz monzonite or monzogranite in most areas, and a complex of Paleocene dikes, stocks, and plutons. The Mesozic rocks and one of the Paleocene units, the Sierrita Granite, form the resistant central core of the range. The northern piedmont, a small portion of which is exposed in the northeast corner of the map, is underlain by the Paleocene (63-64Ma) Ruby Star Granodiorite.

Porphyry copper-molybdenum mineralization associated with emplacement of the Paleocene plutonic rocks has been exploited at three major open-pit mines in the eastern Sierrita Mountains for nearly 50 years. These deposits, from north to south the Pima - Mission, Twin Buttes, and Sierrita – Esperanza, constitute the Pima Mining District. The district, which is still in production, has yielded over 18 billion pounds of copper, 290 million pounds of molybdenum, and considerable lead, zinc, and silver (Keith et al., 1983; Arizona Department of Mines and Mineral Resources file data). Most previous geologic studies in the Sierrita Mountains focused on these three deposits (e.g., Kinneson, 1966; Aiken and West, 1978; West and Aiken, 1982; Barter and Kelley, 1982; Jansen, 1982; Preece and Beane, 1982; Jensen, 1998; Herrmann, 2001).

The largest open-pit mine, the Sierrita-Esperanza, lies in the northeast corner of the map area. An inset map shows our interpretation of the pre-mine geology based on the mapping of Lynch (1967) and Cooper (1973). Mineralization at Sierrita-Esperanza is localized along the intrusive contact zone between the Ruby Star Granodiorite and country rocks. The contact zone is marked by a complex suite of Late Cretaceous through Paleocene dikes, stocks and intrusive breccia. Most of these rocks postdate emplacement of the Ruby Star Granodiorite, but a NNW-trending chain of fine-grained biotite-hornblende diorite stocks was emplaced just prior to intrusion of the Ruby Star. The chain of diorite stocks (TKd) extends across the core range (Johnson et al., 2003), and at least one of these contains small (<2m) comagmatic blebs of medium-grained granodiorite similar in appearance to the Ruby Star. The largest diorite stock, located in the northwest corner of the Sierrita pit, provided an excellent host for mineralization. Other important host rocks include mafic volcanics (Ja), the Harris Ranch Monzonite (Jh), and the Sierrita Breccia (Tsb), an andesitic matrix intrusive breccia (Lynch, 1966; 1967; 1968; Smith, 1975; West and Aiken, 1982).

The Red Boy Rhyolite and Red Boy Peak caldera complex

The central core range of the Sierrita Mountains is dominated by two rock units; the Red Boy Rhyolite, a southeast-tilted (35-60^{o}) cauldron-filling ash-flow tuff, and its

probable sub-caldera pluton, the 177Ma (Riggs et. al, 1993) Harris Ranch Monzonite. A keel-shaped segment of the Red Boy Rhyolite's source cauldron, herein named the Red Boy Peak cauldron, is preserved striking NE-SW across the crest of the range. The keel is formed by two inwardly dipping contacts; a SE-dipping (40-50^{o}) basal contact interpreted as the caldera floor in the northwest, and a gently WNW-dipping, highly irregular buttress unconformity, interpreted as a NW-facing caldera wall that strikes south, parallel to Ox Frame Canyon and forms an outlier at Lobo Peak in the north-central part of the map area. At the base of the keel, a NW-side-down caldera-margin fault zone is inferred (cross-section A-A'' and B-B').

The Red Boy Rhyolite is a moderately phenocryst-rich ash-flow tuff containing subequal amounts of quartz (1-4mm), plagioclase (1mm), and potassium feldspar (1-3mm). Biotite is notably absent or very sparse throughout, except at the top (south of Lobo Peak) where biotite-rich rhyolitic (Jbb) and dacitic (Jbd) welded ash-flow tuff lenses are interleaved with normal Red Boy Rhyolite (Jb). This complex sequence, which also includes a thin andesitic conglomerate lens (Jbc), was interpreted by Cooper (1973) as part of the older Ox Frame volcanics. Ash-flow tuff matrix megabreccia (Jbx) and mesobreccia (Jbz) make up a large portion of the Red Boy Rhyolite caldera-fill. Most of the megaclasts are of Ox Frame rhyolite and andesite lava, but the caldera fill also includes large blocks and lithic swarms of a distinctive 15-20% quartz, plagioclase, potassium feldspar porphyritic rhyolite (Jrp). Although minor dike swarms of the rhyolite porphyry unit (Jrp) are present in pre-caldera rocks just to the north of the map area (Johnson et al., 2003), we recognized no exposures of lava flows or dome-complexes matching this unit anywhere else in the Sierrita Mountains. The rhyolite porphyry (Jrp) is interpreted as an extensive dome complex that was active just prior to and possibly during eruption of the Red Boy Rhyolite. We believe that the dome complex was obliterated and entrained as mega lithic blocks, some of which may have been partially molten, during formation of the Red Boy Peak cauldron.

Ox Frame volcanics and Mesozoic deformation

Red Boy Rhyolite, consistently tilted to the southeast throughout the Sierrita Mountains overlies, with angular unconformity, two distinct packages of volcanic rocks. To the northeast lies an andesite-rhyolite lava succession with interbedded quartz sandstone (chiefly map units Ja, Jr, and Jq) known as the Ox Frame volcanics (Cooper, 1971; 1973). To the south and west lies a thick pile of andesitic lava (Jau), andesitic conglomerate (Jc), and phenocryst-rich dacitic tuff (Jt) that had previously been correlated with the Cretaceous Demetrie Andesite (Kd) of Cooper (1973). The NNW-striking contact that separates the two packages is exposed in the floor and in the wall of the Red Boy Peak caldera. In the floor, the contact (where map unit Jc overlies map unit Jg in the northwest corner of the map) is interpreted as a SW-facing buttress unconformity that overlies a degraded, west-side-down fault scarp. The southerly continuation of the contact is within the upthrown caldera wall block to the southeast, and is therefore at a deeper structural level. The deeper segment, mapped just east of Lobo Peak, is interpreted as an irregular fault surface whose dip and kinematics are poorly understood. Easterly dips ranging between 30^{o} and 80^{o} are observed within a short length of the fault north of Lobo Peak. We tentatively interpret the fault as a steeply NE-dipping reverse fault, possibly reactivated as, or originating as, a strike-slip fault. The

strike-slip interpretation is highly speculative, and is based on the presence of an aphyric to phenocryst-poor rhyolite ash-flow tuff and tuff matrix megabreccia, herein named the tuff of San Juan Wash (Jsj and Jsx) that underlies the andesitic conglomerate (Jc) unit to the west of the fault near George Tank along the west edge of the map area. This ash-flow tuff and the distinct pink to red quartz sandstone and silty mudstone lithic blocks contained in its megabreccia show no affinity to any volcanic unit in the Ox Frame volcanics to the northeast.

The NW-striking fault is truncated by an angular unconformity at the base of the Red Boy Rhyolite. Its >177Ma age and parallelism with a series of contractional faults and folds mapped within Paleozoic rocks directly to the east (Cooper, 1973; Jansen, 1982) and west (Drewes and Cooper, 1973) of this map area lends credence to previous interpretations of an important pre-Laramide, post-Paleozoic structural event in the Sierrita Mountains (McCurry, 1971; Barter and Kelly, 1982; Jansen, 1982). It is important to note, however, that the pre-Laramide event suggested by these workers is based primarily on the presence of an angular unconformity they describe at the base of (rather than within) the Mesozoic section. It is also important to note that the existence of this basal Mesozoic angular unconformity has not been substantiated by recent mapping in the eastern Sierrita Mountains (Richard et al., 2003).

Further complexities to the Mesozoic volcanic history of the Sierrita Mountains are recorded in the Ox Frame volcanics. A north-dipping, rhyolite ash-flow tuff matrix megabreccia herein named and defined as the tuff of George Tank occurs within or overlaps the Ox Frame volcanics below the floor of the Red Boy Peak cauldron in the northwest corner of the map area. The tuff of George Tank is similar to the Red Boy Rhyolite in that it contains 10-25% phenocrysts of quartz (0.5-2mm), plagioclase (1-4mm), and potassium feldspar (0.5-2mm), but it also contains sparse biotite phenocrysts throughout, its quartz phenocrysts are much smaller, and its potassium feldspar content is much lower than in the Red Boy Rhyolite. The northern contact of the tuff of George Tank is interpreted as a south-facing buttress unconformity, and possibly yet another caldera margin.

Horse Pasture Hill unconformity or anticline?

Throughout the northern (Johnson et al., 2003) and central Sierrita Mountains, the Ox Frame volcanics from a consistently NNW dipping (10-30^{o}) homocline. To the south, northerly tilts gradually decrease to ~10^{o}, and at Horse Pasture Hill, dips flip abruptly to the south (30-40^{o}) across a poorly exposed contact we interpret as an angular unconformity. We interpret rocks to the south of this contact as a southerly continuation of a SE-dipping Red Boy Rhyolite and megabreccia sequence (Jb and Jbx). Our interpretaion is strongly influenced by the gently north-dipping orientation of a pair of thin, bedded intervals (Jq and Jrt) within a thick pile of phenocryst-poor Ox Frame rhyolite (Jrl) on the southwest slope of Horse Pasture Hill. The units lie in an area where the tilt pattern would be difficult to explain by folding. On the other hand, the final orientation of any bedded sequence within a rhyolite lava dome complex can be highly erratic. The megabreccia sequence (Jbx) at Horse Pasture Hill includes large areas of coarse-grained megabreccia. This is somewhat unusual because megabreccia blocks in excess of 50m (like the ones at Horse Pasture Hill) are probably not ballistic (eg. Wright and Walker, 1977) and they were most likely deposited as avalanche blocks. The

problem is that the avalanche blocks lie to the southeast of, and therefore, outside the caldera. It is possible, however, that additional syn-volcanic scarps in this area may have been the source of the megablocks.

An alternative interpretation for the south-dipping megabreccia sequence at Horse Pasture Peak is that it lies in the south limb of an E-W striking anticline and that it is part of the Ox Frame volcanics. In this interpretation the megabreccia would correlate either with a pair of thin layers of rhyolite ash-flow tuff (Jtq) mapped within the Ox Frame volcanics just to the north, or with the tuff of George Tank, the megabreccia unit found below the floor of the Red Boy Peak cauldron in the northwest corner of the map. In support of this interpretation, study of the megabreccia at Horse Pasture Hill reveals that the tuff matrix contains small quartz phenocrysts (0.5-2mm), high plagioclase to potassium feldspar phenocryst ratios, and sparse biotite. These observations suggest that the phenocryst mineralogy of the tuff at Horse Pasture Hill is more akin to the older Jurassic tuffs (Jtq or Jg) than the Red Boy Rhyolite (Jb). An intriguing possibility of this alternative interpretation is that the proposed anticline at Horse Pasture Hill has analogues to the east and west. To the west it might connect with the anticline that folds the Jc and Jt units just south of George Tank along the western edge of the map area (note that the fold axis should be offset to the northwest about 3km due to down-to-the northwest motion along the intervening Red Boy Peak caldera-margin fault zone). In the northeast corner of the map, placing a broad, southwest-plunging anticline in the vicinity of the Sierrita mine office complex is a possible explanation for opposing dips in the Ox Frame volcanics in this area.

The Demetrie problem

A Cretaceous sequence of andesitic to dacitic plagioclase-porphyritic lavas called the Demetrie volcanics (Cooper, 1971; 1973) is mapped to the south and east of the Sierrita-Esperanza mine. This sequence retains its Cretaceous age assignment due primarily to stratigraphic relationships described to the east where Spencer et al. (2003) and Richard et al. (2003) show the base of the Demetrie overlying a sequence of feldspathic sandstone and conglomerate correlated with the Lower Cretaceous Bisbee Group. Although obscured by Cenozoic cover, we show a tentative connection between the Demetrie volcanics and the SE-dipping Jurassic volcanic section at Horse Pasture Hill. A thin sequence of andesitic lava (Kd) and a hypabyssal andesite stock (Kdi) is shown overlying the Horse Pasture sequence.

Summary and suggestions for continued work

The geologic history of the Sierrita Mountains is highly complex. Strong alteration of a complex sequence of Mesozoic volcanics intruded by a complex suite of plutonic rocks makes interpreting the geology very difficult. Our work has revealed two major stratigraphic errors that had perpetuated for nearly 50 years in the area. First, Red Boy Rhyolite is older, not younger, than the Harris Ranch Monzonite, and second, the Sierrita Granite, once thought to be Jurassic in age, is now known to be younger than the Paleocene Ruby Star Granodiorite. Our observations also indicate that the Red Boy Peak cauldron margin faces northwest instead of southeast as shown by Fridrich (1991), and Lipman and Fridrich (1990). A significant conclusion regarding these observations is that the sub-caldera pluton for the Red Boy Rhyolite is the Harris Ranch Monzonite and

the Paleocene Ruby Star Granodiorite is so much younger that it can not be related. This observation is perhaps more in keeping with theoretical arguments that porphyry-copper mineralization is related exclusively to intermediate composition, subduction-related magmatism beneath stratovolcanoes (Sillitoe, 1973).

Continued unraveling of the geologic history in this complex range will depend on U-Pb geochronology of several key volcanic units. Dating of the Ox Frame volcanics, which has proved notoriously difficult because of the phenocryst-poor nature of its felsic volcanic rocks (Riggs, written communication) might be accomplished by focusing dating efforts on a series of moderately phenocryst-rich ash-flow tuffs; the tuff of George Tank (Jg), a pair of thin units mapped east of Ox Frame Canyon (Jtq), and a crystal-rich, plagioclase-biotite dacite tuff (Jt) that underlies the Red Boy Rhyolite in the west. Other key units to date include the tuff at Horse Pasture Hill, which we have correlated with the Red Boy Rhyolite, and a pair of rhyolite ash-flow tuffs interbedded within the Demetrie volcanics (Kdlr, and Kdr).

A reliable date on the Harris Ranch Monzonite is critical. Since no sample location is known, it is possible that the 177Ma date reported by Riggs et al. (1994) may not apply to the pluton we have mapped as the Harris Ranch. It is also possible that the 177Ma date reflects the age of zircons inherited from the Ox Frame volcanics. A Cretaceous age for the Harris Ranch is still considered a strong possibility for several reasons. If the Harris Ranch Monzonite were Late Cretaceous it could then be considered part of the extensive plutonic complex of the northern Sierrita Mountains that includes Ruby Star Granodiorite, Sierrita Granite, and the fine-grained diorite stocks (TKd). This entire suite might therefore represent a sub-caldera intrusive complex. The Red Boy Rhyolite has long been considered a Late Cretaceous unit (Cooper, 1973, Lipman and Fridrich, 1990), and an upper Cretaceous age for the major angular unconformity at its base would allow older contractional structures in the Sierritas to be Laramide in age. This would refute rather than support the early Mesozoic orogeny interpretation advanced by previous workers, but which has been questioned due to lack of evidence (Richard et al., 2003). Another problem is that there is no evidence that the Upper Cretaceous Demetrie volcanics are significantly younger than the Red Boy Rhyolite or the Harris Ranch. In fact, the Demetrie volcanics were originally thought to underlie the Red Boy Rhyolite (Copper, 1973). A nonconformity at the base of the Demetrie has not been described, and clasts of Harris Ranch have not been found within its conglomeratic units. In the northerly adjacent Samaniego Peak quadrangle (Johnson et al., 2003) the interaction of intrusive relationships and a series of EW-striking, south-side-down normal faults that are interpreted to have been active during and shortly after formation of the Red Boy Peak caldera strongly suggests that the Harris Ranch Monzonite is closely related in age with the other plutonic units of that area. For instance, the Ash Creek fault cuts older phases of the Harris Ranch Monzonite and a stock of the fine-grained diorite (TKd), but to the east the fault is intruded by the main phase of the Harris Ranch Monzonite and the Sierrita Granite. These relationships suggest that the intrusive rocks were emplaced during a short interval of time and that they might all be related to a single magmatic episode.

Acknowledgments

Special thanks are extended to Phelps Dodge Corporation and the personnel at Sierrita-Esperanza Mine. Mine geologists Dan Aiken and Greg Baugh helped us extensively with tours of the mine, many helpful discussions, and by sharing their time, office space, and other important resources. Mine engineer Russell Hewlitt helped us sort out problems with generating the modern mine topography for our final map. We also would like to thank Matt Turner, James Horton, Walter Harrison, and all the people at Caterpillar Corporation's Demonstration Center and Proving Ground. Kyle Best of the Marley Cattle Company helped us with questions regarding access to areas of the southern piedmont. Norman Harris, Shelly Fox and the people of Sierrita Mining and Ranching helped us extensively with access, logistical support, and scientific information in the core range. We also thank Jon Spencer, Steve Richard, Ann Youberg, Bill Stavast, Eric Seedorff, Mark Barton, and Nancy Riggs for helpful discussions.

Table 1 Major element geochemistry of Cenozoic and Mesozoic volcanic and hypabyssal rocks from the Sierrita Mountains.
The samples were crushed in a steel jaw crusher, split, and ground in a Tema mill using a WC grinding set.
The samples were fused into glass discs and analyzed on a Phillips wavelength dispersive x-ray fluorescence spectrometer for major elements. A separate split of the samples was used to loss on ignition gravimetrically.

Sample	SiO2	TiO2	Al2O3	Fe2O3-T	MnO	MgO	CaO	K2O	Na2O	P2O5	LOI	Total	unit	Ba
	wt. %	wt. %	wt. %	wt. %	wt. %	wt. %	wt. %	wt. %	wt. %	wt. %	wt. %	wt. %		ppm
CAF-2-4941	61.34	1.08	16.36	5.24	0.06	1.69	3.96	4.30	4.58	0.44	0.72	99.76	Ja	1346
CAF-2-4942	74.18	0.25	13.96	1.31	ND	0.13	0.11	5.76	3.76	0.04	0.61	100.11	Jr	947
CAF-2-3829	56.20	0.97	17.49	6.98	0.09	3.29	6.45	2.31	3.62	0.26	1.78	99.44	Ta	756
CAF-2-3849	62.39	0.77	16.39	4.73	0.07	1.65	4.02	3.95	3.68	0.29	1.48	99.42	Tdh	924
CAF-2-3855	66.10	0.46	15.95	2.96	0.05	0.78	2.84	4.04	3.81	0.13	2.55	99.67	Tdx	826
CAF-2-3870	65.66	0.45	16.06	2.88	0.05	0.77	2.88	4.07	3.86	0.13	2.34	99.15	Tdx	838
CAF-2-3917	65.70	0.46	15.80	2.89	0.05	0.79	2.89	4.23	3.49	0.14	3.52	99.95	Tdx	916
CAF-2-3977	63.81	0.70	16.43	4.37	0.06	1.66	4.14	3.36	3.79	0.26	1.01	99.59	Tdh	977
CAF-2-3984	65.69	0.46	15.99	2.91	0.04	0.84	2.85	4.14	3.50	0.13	3.37	99.93	Tdx	812
CAF-2-3990	63.42	0.58	16.27	4.03	0.06	2.24	4.42	2.77	3.60	0.13	2.20	99.72	Tdf	715
CAF-2-4003	63.44	0.59	16.33	4.04	0.07	2.24	4.45	2.67	3.72	0.14	1.60	99.28	Tdf	738
CAF-2-4035-CM1	64.66	0.57	15.99	3.66	0.06	1.48	3.64	3.56	3.66	0.20	1.86	99.34	Tdh	1021
CAF-2-4035-CM2	64.91	0.57	15.95	3.71	0.06	1.48	3.64	3.59	3.66	0.20	1.86	99.63	Tdh	1048
CAF-2-4035-CM3	64.70	0.57	15.98	3.68	0.06	1.48	3.62	3.54	3.65	0.20	1.86	99.34	Tdh	1044
CAF-2-4174	60.86	0.67	16.46	5.04	0.09	0.87	3.51	3.73	3.87	0.27	4.81	100.18	Kd	983
CAF-2-5134	61.84	0.61	16.85	4.10	0.06	1.66	5.47	2.92	3.49	0.15	3.03	100.18	Tdfl	739
CAF-2-5137	58.63	1.02	17.97	5.38	0.06	2.03	5.21	2.44	3.68	0.29	3.34	100.04	Ta	849
CAF-2-5154	63.58	0.61	16.42	4.24	0.06	2.20	4.72	2.96	3.41	0.14	1.89	100.23	Tdf	699
CAF-2-5164	64.23	0.60	16.91	4.11	0.06	0.87	3.89	3.67	3.89	0.26	1.04	99.53	Tdf	1086
CAF-2-5202	51.54	1.62	15.55	10.41	0.14	5.26	7.80	2.18	3.12	0.68	1.84	100.14	Tbu	2241
CAF-2-5207	63.65	0.76	16.02	4.82	0.08	1.66	4.10	3.51	3.87	0.26	0.81	99.54	Tdb	1164
CAF-2-5212	52.71	1.34	15.59	8.87	0.12	5.23	7.87	2.35	3.56	0.54	1.51	99.70	Tbu	986
CAF-2-5213	52.37	1.61	15.92	10.30	0.14	5.13	7.63	2.23	3.40	0.68	0.63	100.04	Tbu	961

Table 1 continued

Sample	SiO2	TiO2	Al2O3	Fe2O3-T	MnO	MgO	CaO	K2O	Na2O	P2O5	LOI	Total	unit	Ba
	wt. %	wt. %	wt. %	wt. %	wt. %	wt. %	wt. %	wt. %	wt. %	wt. %	wt. %	wt. %		ppm
CAF-2-5216	62.78	0.64	15.86	4.46	0.07	2.08	4.15	3.67	3.46	0.24	1.65	99.06	Tdb	1048
CAF-2-5221	52.40	1.34	16.22	8.70	0.10	4.24	7.01	2.56	3.70	0.46	2.54	99.27	Tb	848
CAF-2-5228	54.00	1.16	19.13	7.98	0.08	1.29	6.17	3.60	4.16	0.48	1.88	99.93	Tb	1106
CAF-2-5240	57.06	0.78	17.26	5.37	0.08	2.52	5.82	2.30	3.39	0.27	4.34	99.19	Tbb	1058
CAF-2-5261	53.53	1.05	16.58	7.54	0.10	3.93	6.67	3.02	3.47	0.36	3.32	99.56	Tb	952
CAF-2-5277	55.84	1.05	17.48	7.50	0.11	1.74	4.94	2.85	3.45	0.45	3.76	99.17	Tb	901
CAF-2-5294	54.56	1.07	17.80	7.37	0.11	2.12	6.35	2.60	4.01	0.45	2.56	99.01	Tb	989
CAF-2-5296	51.12	1.24	17.22	10.47	0.11	4.71	8.15	1.75	2.89	0.33	1.48	99.47	Jai	866
CAF-2-5336	74.97	0.23	12.67	1.80	ND	0.11	0.05	6.88	2.25	0.03	0.56	99.54	Jrl	915
CAF-2-5343	65.39	0.64	15.75	4.09	0.08	1.09	2.43	4.89	4.27	0.21	1.02	99.86	Jh	1030
CAF-2-5360	75.84	0.26	13.29	0.25	ND	0.04	0.07	7.76	2.42	0.03	0.31	100.27	Jr	731
CAF-2-5362-CM2	76.31	0.24	13.20	1.04	0.02	0.03	0.60	2.26	5.51	0.03	0.68	99.92	Jrl	239
CAF-2-5362-CM3	75.72	0.24	13.09	1.06	0.02	0.02	0.60	2.24	5.68	0.03	0.68	99.38	Jrl	216
CAF-2-5639	55.93	0.96	17.93	7.82	0.11	2.92	6.63	2.25	3.48	0.29	1.24	99.57	Td	849
CAF-2-5644	74.06	0.25	13.56	1.12	0.03	0.07	0.05	7.21	2.77	0.03	0.65	99.79	Jrl	1083
CAF-2-5695	50.31	1.36	19.11	9.58	0.18	2.97	7.74	3.20	3.44	0.36	0.94	99.19	Ja	1067
CAF-2-5718	56.01	1.19	17.30	8.12	0.16	2.60	5.80	3.01	3.47	0.41	1.33	99.40	Jhm	1165
CAF-2-5746	56.00	1.08	16.81	7.39	0.18	2.09	3.28	3.99	3.53	0.40	4.64	99.39	Ja	1460
CAF-2-5897	66.22	0.58	15.62	3.83	0.11	1.12	2.51	4.57	4.08	0.20	0.85	99.69	Kh	945
CAF-2-5943	65.21	0.49	15.81	4.08	0.11	1.37	2.26	1.54	5.56	0.17	2.56	99.17	Jau	660
CAF-2-5945-CM1	52.43	0.94	17.17	6.87	0.13	2.31	6.08	0.24	7.59	0.25	5.01	99.02	Jau	131
CAF-2-5945-CM2	52.63	0.94	17.16	6.83	0.13	2.32	6.15	0.23	7.48	0.25	5.01	99.13	Jau	104
CAF-2-6048	54.88	1.08	17.27	6.36	0.09	2.86	6.94	2.81	3.56	0.46	3.55	99.86	Tb	1216
CAF-2-6076	71.53	0.40	14.44	2.53	0.02	0.26	0.18	6.00	2.84	0.09	1.03	99.32	Jg	1078
CAF-2-6401	56.85	1.14	16.50	7.69	0.13	2.43	4.02	4.31	4.28	0.41	1.28	99.05	Ja	1666
CAF-2-6622	53.29	1.15	17.70	9.09	0.16	4.07	7.23	2.04	3.51	0.30	1.16	99.71	Td	699
CAF-2-6680	51.16	1.12	15.29	7.33	0.10	3.59	5.75	2.44	4.47	0.39	7.37	99.00	Tm	759

Table 1 continued

Sample	SiO2	TiO2	Al2O3	Fe2O3-T	MnO	MgO	CaO	K2O	Na2O	P2O5	LOI	Total	unit	Ba
	wt. %	wt. %	wt. %	wt. %	wt. %	wt. %	wt. %	wt. %	wt. %	wt. %	wt. %	wt. %		ppm
CAF-2-6689	70.29	0.38	15.49	2.62	0.05	0.80	2.26	3.68	4.05	0.13	0.32	100.06	Tgd	959
CAF-2-6694-CM1	75.08	0.20	13.51	1.62	0.07	0.20	0.68	5.02	3.77	0.06	0.25	100.46	Tg	511
CAF-2-6694-CM2	74.86	0.20	13.54	1.64	0.07	0.20	0.68	4.96	3.75	0.06	0.25	100.21	Tg	511
CAF-2-6710	69.52	0.34	14.66	2.68	0.07	0.90	2.48	4.49	3.42	0.09	0.44	99.09	Tgd	658
1-2-03-8	59.17	0.69	17.74	6.03	0.12	2.39	4.22	3.34	4.04	0.36	2.67	100.77	Kd	1042
1-3-03-1	77.02	0.17	13.29	1.16	0.05	0.33	1.02	3.49	3.54	0.04	0.81	100.91	Kdlr	950
1-3-03-2	56.68	0.98	18.46	8.26	0.11	2.82	4.69	2.83	4.00	0.29	1.44	100.56	Kd	1012
1-8-03-8	57.59	0.87	17.75	7.12	0.12	2.55	5.08	3.02	4.01	0.38	2.03	100.52	Kd	1071
1-10-03-3	59.22	0.63	16.48	5.65	0.11	1.42	4.55	3.62	3.84	0.29	4.33	100.14	Tx(Kd)	1007
1-15-03-3	67.03	0.51	16.09	2.94	0.02	0.69	3.00	4.25	4.03	0.19	1.73	100.49	Tad	869
1-16-03-1	57.92	1.38	18.34	5.71	0.05	1.48	5.78	3.17	4.03	0.39	2.21	100.47	Tap	754
1-29-03-3-CM2	39.24	0.03	0.99	28.27	0.55	ND	30.18	0.02	0.07	0.26	0.16	99.77	skarn	ND
1-29-03-3-CM3	39.20	0.03	0.99	28.36	0.56	ND	30.15	0.02	0.07	0.26	0.16	99.79	skarn	ND
3-28-03-1	74.83	0.32	14.74	0.65	0.00	0.06	0.20	6.15	3.37	0.05	0.60	100.97	Jt	1414
4-18-03-1	59.02	0.97	16.45	7.07	0.09	3.39	5.93	2.79	3.70	0.30	0.79	100.50	diorite	934
12-3-02-1	59.30	0.97	18.04	6.18	0.09	2.77	6.15	2.56	3.71	0.24	0.82	100.83	Ta	856
12-4-02-1	59.63	0.67	17.13	5.13	0.09	1.79	2.64	3.88	4.46	0.25	5.10	100.77	Kd	1094
12-5-02-1-CM1	61.57	0.62	16.52	5.16	0.08	2.20	2.68	3.42	4.53	0.28	3.56	100.63	Kd	872
12-5-02-1-CM2	61.73	0.63	16.55	5.18	0.09	2.21	2.69	3.43	4.53	0.28	3.56	100.88	Kd	876
12-6-02-2	73.49	0.15	13.69	1.10	0.07	0.26	0.92	6.13	2.70	0.04	0.73	99.27	Kdlr	910
12-9-02-1	58.25	0.94	18.07	6.10	0.08	2.93	6.26	2.09	3.86	0.25	1.81	100.65	Ta	784
12-10-02-4	65.52	0.66	16.28	4.71	0.07	1.15	4.05	3.30	3.99	0.25	0.70	100.68	Tdh	1087
12-10-02-8-CM1	57.88	1.03	17.99	6.80	0.09	3.22	6.57	2.28	3.72	0.30	0.68	100.56	Ta	831
12-10-02-8-CM2	57.80	1.02	18.00	6.79	0.09	3.21	6.55	2.29	3.71	0.30	0.68	100.45	Ta	837
12-10-02-8-CM3	57.53	1.02	17.93	6.75	0.09	3.20	6.52	2.25	3.71	0.30	0.68	99.98	Ta	851
12-11-02-7	65.39	0.63	15.97	4.51	0.06	1.56	4.01	3.28	4.00	0.20	1.07	100.68	Tdh	988

Table 1 continued

Sample	SiO2	TiO2	Al2O3	Fe2O3-T	MnO	MgO	CaO	K2O	Na2O	P2O5	LOI	Total	unit	Ba
	wt. %	wt. %	wt. %	wt. %	wt. %	wt. %	wt. %	wt. %	wt. %	wt. %	wt. %	wt. %		ppm
BJJ-785	76.39	0.16	12.86	1.21	0.03	0.13	0.17	3.70	5.13	0.04	0.65	100.47	Tg	372
BJJ-793	57.96	1.16	17.19	7.18	0.17	2.24	4.36	4.61	3.45	0.42	1.59	100.33	Ja	1315
BJJ-800	71.75	0.38	14.25	2.14	0.08	0.41	0.91	3.85	5.35	0.09	0.91	100.13	Jh	1149
BJJ-805	73.00	0.38	14.26	1.92	0.05	0.43	0.49	3.95	5.32	0.11	1.04	100.95	Jh	1146
BJJ-824-1	68.85	0.55	15.79	2.52	0.02	0.55	0.61	4.61	6.26	0.14	0.72	100.61	Jri	1287
BJJ-844	59.73	0.70	17.02	6.33	0.15	2.77	4.26	3.67	2.73	0.25	2.53	100.14	Jau	1186
BJJ-847	71.83	0.34	13.68	2.11	0.06	0.48	0.92	3.26	5.71	0.08	1.09	99.56	Jh	742
BJJ-850	71.29	0.41	14.26	2.34	0.05	0.50	1.22	3.54	5.69	0.11	0.51	99.92	Jh	886
BJJ-851	59.35	0.84	17.64	6.45	0.10	2.41	5.54	4.06	2.79	0.31	0.52	100.01	Td	952
BJJ-853	68.53	0.47	15.74	3.11	0.04	1.05	3.29	4.02	3.62	0.11	0.91	100.89	Tdf	931
BJJ-857	65.27	0.55	16.03	3.76	0.06	2.02	4.06	3.67	3.29	0.13	1.48	100.31	Tdf	768
BJJ-933	54.55	1.27	16.69	7.10	0.14	2.59	3.57	5.68	3.83	0.42	4.11	99.95	Tm	1400
BJJ-934	50.30	1.01	15.22	7.33	0.13	5.27	5.40	4.00	3.70	0.37	6.84	99.57	Tm	792
BJJ-938-CM1	78.22	0.06	12.84	0.46	ND	ND	0.38	3.97	4.55	0.02	0.23	100.73	Tgf	ND
BJJ-938-CM2	78.00	0.06	12.72	0.51	ND	0.04	0.38	3.97	4.55	0.02	0.23	100.47	Tgf	ND
BJJ-938-CM3	77.54	0.06	12.74	0.50	ND	0.01	0.37	3.99	4.54	0.02	0.23	100.00	Tgf	ND
BJJ-957	64.21	0.53	16.66	3.30	0.05	1.38	3.84	4.83	2.51	0.19	2.98	100.48	Tdxi	867

All values are in weight percent, except for Ba, which is in parts per million.
Fe2O3-T is total iron expressed as Fe2O3.
LOI is loss on ignition.
Samples with the extension -CM1, -CM2, and -CM3 are replicates.
ND is below the lower limit of determination.

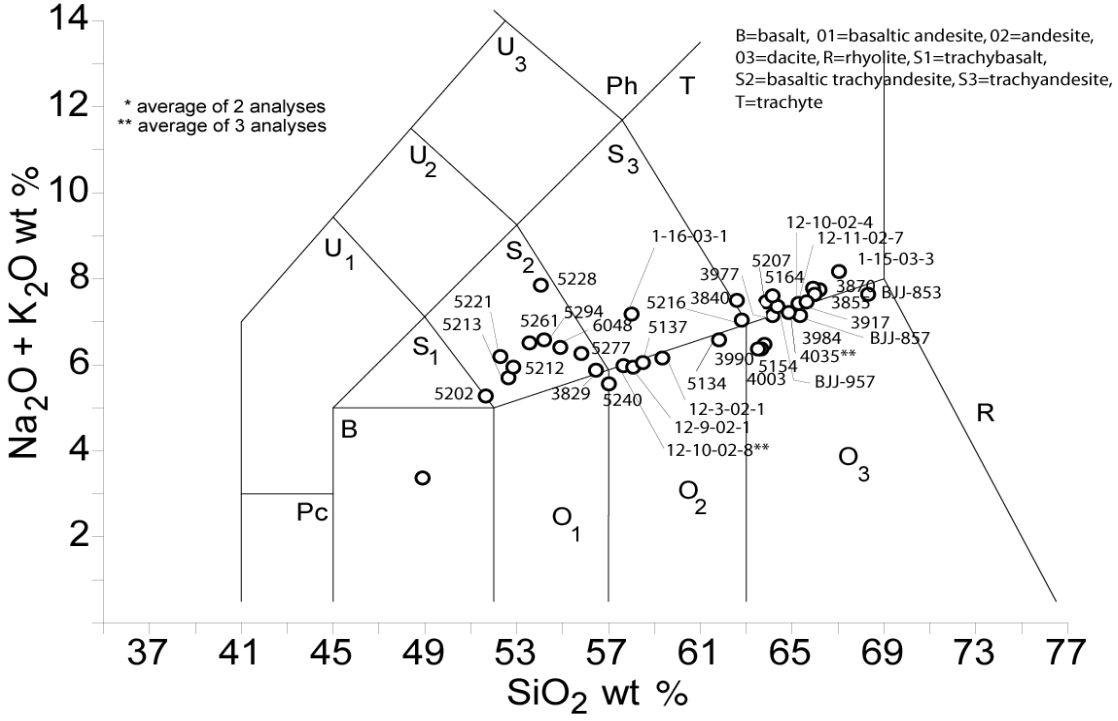

Figure 1 Total alkali versus silica diagram of Le Bas et al. (1986) showing analyses of Mid-Tertiary volcanic and hypabyssal rocks from the Tinaja Peak and Batamote Hills volcanic fields of the southern Sierrita Mountains. Complete analyses shown in Table 1.

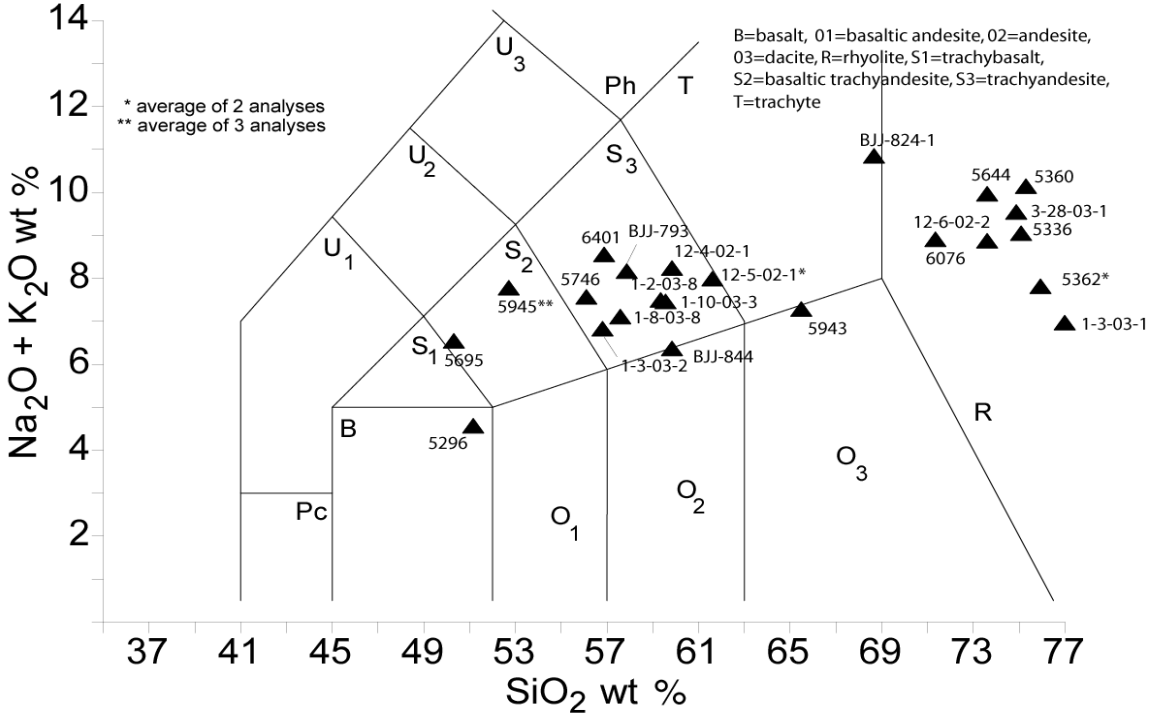

Figure 2 Total alkali versus silica diagram of Le Bas et al. (1986) showing analyses of Mesozoic volcanic and hypabyssal rocks of the central Sierrita Mountains. Complete analyses shown in Table 1.

References

Aiken, D.M., and West, R.J., 1978, Some geologic aspects of the Sierrita-Esperanza copper-molybdenum deposit, Pima County, Arizona, in Jenney, J.P., and Hauck, H.R., eds., Proceedings of the Porphyry Copper Symposium, Tucson, Ariz., March 18-20, 1976: Arizona Geological Society Digest, v. 11, p. 117-128.

Barter, C.F., and Kelly, J.L., 1982, Geology of the Twin Buttes mineral deposit, Pima mining district, Pima County, Arizona, in Titley, S.R., ed., Advances in geology of the porphyry copper deposits, southwestern North America: Tucson, University of Arizona Press, p. 407-432.

Cooper, J. R., 1960, Some features of the Pima mining district, Pima County, Arizona: U.S.Geological Survey Bulletin 1112-Calcareous, p. 63-103.

Cooper, J.R., 1971, Mesozoic stratigraphy of the Sierrita Mountains, Pima County, Arizona: U.S. Geological Survey Professional Paper 658-D, 42 pp.

Cooper, J.R., 1973, Geologic map of the Twin Buttes Quadrangle, southwest of Tucson, Pima County, Arizona: U.S. Geological Survey Miscellaneous Geological Investigations Map I-745, scale 1:48,000.

Damon, P.E., and Bikerman, M., 1964, Potassium-argon dating of post-Laramide plutonic and volcanic rocks within the Basin and Range province of southeastern Arizona and adjacent areas: Arizona Geological Society Digest v. 7, p. 63-78.

Damon, P.E., 1965, Correlation and chronology of the ore deposits and volcanic rocks: Tucson, University of Arizona, U.S. Atomic Energy Commission Annual Report, no. C00-689-50, 60 pp.

Damon, P.E., 1966, Correlation and chronology of the ore deposits and volcanic rocks: Tucson, University of Arizona, U.S. Atomic Energy Commission Annual Report, no. C00-689-60, 46 pp.

Drewes, Harald, and Cooper, J.R., 1973, Reconnaissance geologic map of the west side of the Sierrita Mountains, Palo Alto Ranch quadrangle, Pima County, Arizona: U.S. Geological Survey Miscellaneous Field Studies Map MF-538, 1 sheet, scale 1:24,000.

Fridrich, C.J., 1991, Geologic map of Sierrita caldera fragment, Sierrita Mountains, Pima County, Arizona: Arizona Geological Survey Contributed Map CM-91-L, 1 sheet, scale 1:24,000.

Hermann, M. A., 2001, Episodic magmatism and hydrothermal activity, Pima Mining District, Arizona: Tucson, University of Arizona, M.S. thesis, 44 pp.

Jansen, L.J., 1982, Stratigraphy and structure of the Mission copper deposit, Pima mining district, Pima County, Arizona, *in* Titley, S.R., ed., Advances in geology of the porphyry copper deposits, southwestern North America: Tucson, University of Arizona Press, p. 467-474.

Jensen, P. W., A structural and geochemical study of the Sierrita porphyry copper system, Pima County, Arizona: Tucson, University of Arizona, M.S. thesis, 136 pp.

Johnson, B. J., Ferguson, C. A., and Pearthree, P. A., 2003, Geologic map of the Samaniego Peak 7 ½' Quadrangle, Pima County, Arizona: Arizona Geological Survey Digital Geologic Map DGM-30, scale 1:24,000.

Keith, S.B., Gest, D.E., DeWitt, E., Woode T.N., and Everson, B.A., 1983, Metallic mineral districts and production in Arizona: Arizona Bureau of Geology and Mineral Technology Bulletin 194, 58 p., 1 sheet, scale 1:1,000,000.

Kinnison, J.E., 1966, The Mission copper deposit, Arizona, in Titley, S.R., and Hicks, C.L., eds., Geology of the porphyry copper deposits, southwestern North America: Tucson, University of Arizona Press, p. 281-287.

Le Bas, M. J., Le Maitre, R.W., Streckeisen, A., and Zanettin, B., 1986, A chemical classification of volcanic rocks based on the total alkali-silica diagram: Journal of Petrology, v. 27, p. 745-750.

Lacy, W.C., 1959, Structure and ore deposits of the east Sierrita area, in Heindl, L.A., ed., Southern Arizona Guidebook II, combined with the 2nd annual Arizona Geological Society Digest: Arizona Geological Society, p. 184-192.

Lipman, P.W., and Fridrich, C.J., 1990, Cretaceous caldera systems: Tucson and Sierrita Mountains, *in* Gehrels, G.E., and Spencer, J.E., eds., Geologic excursions through the Sonoran Desert Region, Arizona and Sonora: Arizona Geological Survey Special Paper 7, p. 51-65.

Lynch, D.W., 1966, The economic geology of the Esperanza mine and vicinity, in Titley, S.R., and Hicks, C.L., eds., Geology of the porphyry copper deposits, southwestern North America: Tucson, University of Arizona Press, p. 267-280.

Lynch, D.W., 1967, Geology of the Esperanza mine and vicinity, Pima County, Arizona: Tucson, University of Arizona, M.S. thesis, 70 pp.

Lynch, D.W., 1968, The geology of the Esperanza mine, in Titley, S.R., ed., Southern Arizona Guidebook III: Arizona Geological Society, p. 125-136.

Marvin, R.F., Stern, T.W., Creasey, S.C., and Mehnert, M.H., 1973, Radiometric ages of igneous rocks from Pima, Santa Cruz, and Cochise Counties, southeastern Arizona: U.S. Geological Survey Bulletin 1379, 27 pp.

McCurry, W.G., 1971, Some mineralogy and alteration features at the the Twin Buttes Mine: unpublished paper, presented to Arizona Section, AIME, Mining Geology Division, 9 pp.

Preece, R.K., III, and Beane, R.E., 1982, Contrasting evolutions of hydrothermal alteration in quartz monzonite and quartz diorite wallrocks at the Sierrita porphyry copper deposit, Arizona: Economic Geology, v. 77, no. 7, p. 1621-1641.

Richard, S.M., Spencer, J.E., Youberg, A., and Johnson, B.J., 2003, Geologic map of the Twin Buttes 7 ½' Quadrangle, Pima County, Arizona: Arizona Geological Survey Digital Geologic Map DGM-31, scale 1:24,000.

Reynolds, S.J., Florence, F.P., Welty, J.W., Roddy, M.S., Currier, D.A., Anderson, A.V., and Keith, S.B., 1986, Compilation of Radiometric Age Determinations in Arizona, Arizona Geological Survey Bulletin 197, 258 p., 2 sheets, scale 1:1,000,000.

Riggs, N.R., Hon, K.A., and Haxel, G.B., 1994, Early to Middle Jurassic magmatic arc rocks of south-central and southeastern Arizona, *in* Thorman, C. H. and Lane, D. E. (eds.) USGS Research on Mineral Resources-1994, Part B-Guidebook for field trips, p. 7-14.

Seedorff, E., 1983, Sierrita-Esperanza porphyry Cu-Mo system: Relation to evolution of the Ruby Star batholith as revealed by post-mineral tilting: unpublished report, Palo Alto, CA, Stanford University, 18 pp.

Shafiqullah, M., and Langlois, J.D., 1978, The Pima mining district, Arizona--A geochronologic update, in Callender, J.F., Wilt, J.C., Clemons, R.E., and James, H.L., eds., Land of Cochise, southeastern Arizona: New Mexico Geological Society 29th Field Conference Guidebook, p. 321-327.

Sillitoe, R. H., 1973, The tops and bottoms of porphyry copper deposits: Economic Geology, v. 68, p. 799-815.

Spencer, J.E., Youberg, A., and Ferguson, C. A., 2003, Geologic map of the Esperanza Mill 7 ½' Quadrangle, Pima County, Arizona: Arizona Geological Survey Digital Geologic Map DGM-33, scale 1:24,000.

Smith, V.L., 1975, Hypogene alteration at the Esperanza Mine, Pima County, Arizona: Tucson, University of Arizona, M.S. thesis, 161 pp.

Titley, S.R., 1982, Some features of tectonic history and ore genesis in the Pima mining district, Pima County, Arizona, in Titley, S.R., ed., Advances in geology of the porphyry copper deposits, southwestern North America: Tucson, University of Arizona Press, p. 387-406.

West, R.J., and Aiken, D.M., 1982, Geology of the Sierrita-Esperanza deposit, Pima mining district, Pima County, Arizona, *in* Titley, S.R., ed., Advances in geology of the porphyry

copper deposits, southwestern North America: Tucson, University of Arizona Press, p. 433-465.
Wright, J.V., and Walker, G.P., 1977, The ignimbrite source problem: Significance of a co-ignimbrite lag-fall deposit: Geology, v. 5, p. 729-732.
Williamson, R.L., Jr., and Poulton, M.M., 1995, The geology of the Mineral Hill area, Mission Mine, Pima County, Arizona, *in* Pierce, F.W., and Bolm, J.G., eds., Porphyry copper deposits of the American Cordillera: Arizona Geological Society Digest 20, p. 442-454.

Unit Descriptions for the Batamote Hills 7.5' quadrangle, Pima County, Arizona

(to accompany Arizona Geological Survey Digital Geologic Map DGM-32)

Quaternary

dl Mine dump (<50 years) – Very poorly-sorted, angular rock debris ranging in size from sand to boulders (some up to 3m), but generally in the cobble-boulder size range. The rock debris, derived from Mesozoic and Paleocene volcanic and plutonic rock units, was excavated from the Sierrita-Esperanza open-pit mine and deposited mostly in 5-10m thick sequences defined by horizontal surfaces with intervening angle-of-repose foresets. The dump covers an approximately 7 km^2 area mostly to the south and east of the mine (0-200m thick).

d Disturbed areas (<100 years) – Areas where human activity has obscured the underlying geology, including excavation of earthen water tanks.

Qyc Late Holocene active channel deposits (<100 years) – Unit Qyc consists of braided and meandering active channel deposits. Qyc deposits are composed of coarse to medium sands, pebbles, and cobbles, with occasional boulders. Clasts are typically angular to sub-angular and dominated by volcaniclastic material. Incised meandering channels are high order streams with low order braided channels. Soil formation is minimal to absent for these active channel surfaces. Qyc is primarily vegetated by opportunistic grasses, shrubs, and flood damaged trees.

Qy2 Late Holocene alluvium (<2 ka) – Unit Qy2 consists of recent alluvium on floodplains and low terraces that shows evidence of intermittent inundation during large flood events. Qy2 deposits are composed of sub-rounded to rounded, pebble to cobble, volcaniclastic conglomerate with a sand loam matrix. Qy2 deposits are located along active channels less than 1 m above the active channels. Surfaces are commonly planar. Qy2 soils are weakly developed, 10 YR 5/3 brown to light brown, with no ped development and contain no secondary carbonate. Qy2 is primarily vegetated by acacia trees with rare opportunistic grasses

Qy1 Middle to older Holocene alluvium (~2 to 10 ka) – Unit Qy1 consists of low terraces and mid-channel island deposits composed of sand, silt, and clay, with a dominance of cobbles. Qy1 deposits are located along active channels less than 2 m above the active channels. Surfaces are commonly planar. Qy1 soils are weakly developed, 10 YR 5/3 brown to light brown, with some ped formation. There is minimal clay and no carbonate accumulation. Desert pavement is sparse and immature. Qy1 is primarily vegetated by small mesquite and acacia trees with some opportunistic grasses.

Qy Undifferentiated Holocene alluvium (~100 years to 10 ka)

Ql Late Pleistocene alluvium (~10 to 130 ka) – Unit Ql consists of weakly to moderately dissected alluvial valley fill deposits which commonly flank active channel valley walls. Ql deposits are composed of silt and clay matrix-supported volcaniclastic cobbles. Ql surfaces are lower than Qm surfaces and planar with more dissection and beveling near their eroded edges. Some of the Ql surfaces occur as thin veneers over Tcv deposits. Ql soils are weak to moderately developed, 7.5 YR 4/6 light brown to

yellowish brown, with no carbonate present in the profile, with platy peds and moderate clay accumulation. Ql has a moderately formed desert pavement with no interlocking of the clasts. Ql represents a period of aggradation within valleys which experienced a period of stability expressed in the beveled Tcv deposits. Ql is primarily vegetated by sparse acacia and mesquite trees, barrel cactus, and agave.

Qm Middle Pleistocene alluvium (~130-750 ka) – Unit Qm consists of moderately dissected alluvial fan deposits. The fan deposits dominate the western half of the map area, and have been buried and dissected in the southern portion. Qm deposits are composed of clast-supported, volcaniclastic, cobble conglomerate with clay and silt matrix. There is a ~2 cm eolian loam covering the top of Qm. Qm is beveled with moderate dissection across the entire surface. Qm soils are moderately to strongly developed, 2.5 YR 4/6 orange-red, with no carbonate in the profile, and well developed clay coated medium blocky peds. The desert pavement is moderately developed with some interlocking clasts. Qm represents a major aggradation event that post dated the incision of Tcv. Qm is primarily vegetated by sparse mesquite trees and barrel cactus.

Qc Colluvium and talus (<2 Ma) – Unconsolidated to moderately consolidated colluvium and talus hillslope deposits. This units typically includes subangular to angular, poorly sorted, sand to boulder sized clasts. Adjacent bedrock lithologies dominate the clast compositions. These deposits range in age from Holocene to Pleistocene.

QTs Surficial deposits, undivided (Quaternary to late Tertiary) – Deeply dissected and highly eroded alluvial fan deposits. QTs surfaces are alternating eroded ridges and deep valleys, with ridgecrests typically 10 to 30 meters above adjacent active channels. The thickness of QTs deposits is not known. QTs surfaces are drained by deeply incised tributary channel networks. QTs deposits include very coarse boulder and cobble hillslope deposits, moderately-indurated pebble to cobble conglomerate, fine- to coarse-grained alluvial fan deposits, and buried paleosols.

Mid-Tertiary

Tcv-Ql Pedimented volcaniclastic conglomerate and sandstone (Late Pleistocene ~10 to 130 Ka) – A strath terrace of Late Pleistocene alluvium cut into the Tertiary bedrock along Champurrado Wash.

Tcv Volcaniclastic conglomerate and sandstone (Tertiary) – A heterogeneous volcaniclastic unit consisting of clast-supported, boulder-cobble-pebble conglomerate in the north grading to the south into cobble-pebble, sandy, matrix-supported conglomerate and pebbly sandstone. The unit locally includes pumiceous sandstone beds and rare dacitic pyroclastic beds less than 1m thick with abundant plagioclase, biotite, and hornblende phenocrysts. Bed thicknesses decrease from very thick-bedded to massive in the north to medium- to thick-bedded and thin- to medium-bedded to the south. The unit interfingers with the andesite of Tinaja Hills and the dacite of Tinaja Peak along the northern edge of the Tinaja Hills. Volcanic lithic clasts in the unit represent a diverse suite of Mesozoic and Tertiary lithologies derived from the Tinaja Hills, Batamote Hills and the Sierrita Mountains. In general, volcanic clasts in the north are exclusively Mesozoic, but sparse lenses of conglomerate with Tertiary volcanic clasts also occur in this area. The lowermost portion of this unit (strata that underlie the andesite of Tinaja Hills) is equivalent to the volcanic lithic sandstone

(Tvs) of Spencer et al. (2003) to the east. The volcaniclastic conglomerate and sandstone is at least 500m thick.

Tdh Dacite of Tinaja Peak (Tertiary) – Dacitic lava containing approximately 10% 0.5-2.0mm subhedral to euhedral, rounded, strongly zoned plagioclase, 2-5% 0.5-3.0mm euhedral hornblende, trace to minor amounts of 1mm biotite, and a trace of opaque phenocrysts. Matrix is typically gray and crystalline, with vitric zones near the base. Zones of vitric autobreccia are abundant at the base. Five chemical analyses of this lava show that it is slightly more mafic than the lower dacite of Tinaja Peak (Tdx), and that it straddles the tie between the trachyte and dacite field of Le Bas et al. (1986). With no exposed top, the unit is at least 150m thick at Tinaja Peak.

Tdx Lower dacite of Tinaja Peak (Tertiary) – Dacitic lava containing approximately 20% 1-3.5mm subhedral to euhedral, rounded, strongly zoned plagioclase, 3-5% 0.5-3.0mm hornblende, and traces of 2mm subhedral to euhedral clinopyroxene, <1mm biotite, and <0.3mm opaque phenocrysts. Matrix is typically gray to orange-brown and crystalline. A well-developed vitric autobreccia occurs at the base, but the carapace autobreccia is mostly absent. Four chemical analyses of this lava show that it is slightly more felsic than the dacite of Tinaja Peak (Tdh) and that it lies on the tie between the trachyte and dacite field of Le Bas et al. (1986) (0-100m thick).

Tcx Conglomerate and breccia (Tertiary) – Coarse-grained, angular-clast, oligomict conglomerate and breccia containing clasts of the lower dacite of Tinaja Peak (Tdx, 30-90%), dacite of Escondido Wash (Tdf, 5-40%), and Mesozoic volcanic clasts (10-30%). The unit mostly underlies the lower dacite of Tinaja Peak (Tdx), but also appears to overlap the lava along its eastern margin. The conglomerate and breccia is mostly massive, with a pumiceous, sandy volcaniclastic matrix (0-25m thick).

Tdf Dacite of Escondido Wash (Tertiary) – Dacite lava containing 20-30% 0.3-2.0mm euhedral, zoned plagioclase, and 5-7% 0.2-2mm subhedral to euhedral clinopyroxene. Matrix is typically vitric and very dark, and the lava is massive, displaying rare zones of autobreccia. Chemical analyses of two samples from this unit show it to be a true dacite (0-100m thick).

Ta Andesite of Tinaja Hills (Tertiary) – Phenocryst-poor (0.5-2% < 1mm subhedral plagioclase) massive to vesicular and scoriaceous andesitic lava. The unit occurs as amalgamated flows with abundant flow breccia and reddish weathering scoriaceous zones marking flow contacts. Matrix is typically microcrystalline or strongly devitrified displaying a blotchy, micro-amygdaloidal texture. Chemical analyses of five samples from this unit indicate a composition that straddles the tie between the andesite and trachyandesite field of Le Bas et al. (1986). The unit is up to 200m thick.

Tbu Upper basaltic trachyandesite lava (Tertiary) – Vesicular basalt lava containing ~5% 0.5-2.0mm anhedral olivine and <0.5% <1mm euhedral plagioclase phenocrysts. Three analyses of samples from two exposures of this unit show it to be slightly more mafic and less alkaline than flows of the older basaltic trachyandesite map unit (Tb). The unit is at least 10m thick.

Tds Volcaniclastic sandstone and conglomerate (Tertiary) – Less than 5 meters of sandy matrix, reddish volcaniclastic sandstone and pebble conglomerate (0-10m thick).

Tdb Dacite of Batamote Hills (Tertiary) – Dacitic lava containing 10-15% 0.5-3mm, euhedral, zoned plagioclase and 1-2% 0.5-2mm euhedral hornblende and biotite phenocrysts. To the east, the lava contains 1-5% finely crystalline matrix, irregular clots up to 30cm with <5% 1-2.5mm zoned plagioclase and sparse <.05mm opaques. Mafic phenocrysts in this lava are commonly strongly altered to opaque psuedomorphs. Unaltered mafics are present only in the basal vitric autobreccia. Two analyses of this lava show it to be slightly more alkaline and mafic than other dacite lavas in the area, lying along the tie between the trachyte and trachyandesite fields of Le Bas et al. (1986) (0-200m thick).

Tdt Tuff of Batamote Hills (Tertiary) – Massive, nonwelded dacitic ash-flow tuff containing 10-20% phenocrysts of plagioclase, hornblende, and biotite in similar proportions and size-shape ranges as in the overlying dacite of Batamote Hills (Tdb). The tuff is light tan to peach-colored and locally includes flow unit breaks that define bedding. Lithic lapilli, mostly of basaltic lava, constitute less than 5% of the tuff (0-65m thick).

Ttb Bedded tuff (Tertiary) – Thin- to medium-bedded, nonwelded ash-fall tuff, with rare ash-flow tuff and surge units. The phenocryst assemblage in these tuffs are mostly similar to that of the overlying tuff of Batamote Hills (Tdt), but some of the units are significantly more phenocryst-poor. Basaltic and intermediate lava lithic lapilli along with probable Mesozoic volcanics and granitic fragments make up basalt 5-25% of the pyroclasts. The bedded tuff unit interfingers with several basaltic lava units (Tb and Tbb) and a sandstone and conglomerate (Ts) unit along the western slopes of the Batamote Hills (0-50m thick).

Tb Basaltic trachyandesite lava (Tertiary) – Vesicular basalt lava containing 2-3% 0.5-3.0mm subhedral to anhedral olivine and <1% 1-1.5mm subhedral to euhedral weakly zoned plagioclase, and trace of 1-1.5mm subhedral, glomeroporphyritic clinopyroxene phenocrysts. The basalt lava occurs as several discrete flows that are amalgamated to the north of Peñitas Wash, but to the south interfinger with the bedded tuff (Ttb) and sandstone and conglomerate unit (Ts) along the western slope of the Batamote Hills. Six analyses of samples from separate flows of this unit all lie within the basaltic trachyandesite field of Le Bas et al. (1986). An amalgamated sequence of flows near Batamote Tank is 100m thick, but farther south, individual flows range between 5 and 25m thick.

Tbb Biotite-phyric basaltic andesite lava (Tertiary) – Light gray to green weathering basaltic lava containing 1-2% 1-2mm euhedral to subhedral melt-inclusion, weakly zoned plagioclase, 0.5% 1-2mm biotite, 0.5% <1mm subhedral clinopyroxene phenocrysts, and sparse xenocrysts (?) of olivine up to 6mm (0-30m thick).

Ts Sandstone and conglomerate (Tertiary) - Reddish sandstone, pebbly sandstone and pebble-cobble conglomerate containing clasts of granite, Mesozoic volcanics, and sparse Tertiary volcanics (up to 30m thick).

Th* Helmet Conglomerate (Tertiary) – A heterogeneous sequence of avalanche breccia, conglomerate and sandstone containing clasts derived from a wide variety of Mesozoic and Paleozoic lithologies. Thin interbeds of pumiceous sandstone occur above a distinctive, coarse-grained plagioclase-porphyritic andesite lava marker unit (Tap). Damon and Bikerman (1964) report a biotite K-Ar date of 28.6 $\pm$ 2.6Ma from a tuff

that probably correlates with one of the pumiceous sandstone beds (Richard et al., 2003). The entire sequence of Helmet Conglomerate is at least 2km thick.

Tap* Porphyritic andesite (Tertiary) – Coarse-grained, plagioclase-porphyritic andesite lava (50-100m thick).

* shown on cross-section only

Paleocene

Tmi Mafic dikes (Tertiary) – Fine-grained mafic dikes of probable diorite to monzodiorite in composition with abundant chloritic altered mafic minerals.

Tph Hornblende porphyry dikes (Tertiary) – Fine- to medium-grained monzonite dikes with abundant, euhedral hornblende phenocrysts up to 15mm.

Tpb Biotite porphyry dike (Tertiary) – Fine- to medium-grained monzonite dike with abundant biotite phenocrysts up to 8mm.

Tsb Sierrita Breccia (Tertiary) – Strongly copper and molybdenum-mineralized intrusive breccia mapped in the Sierrita-Esperanza pit. The breccia has a dark-colored matrix of fine-grained biotite and quartz. The breccia includes clasts of country rock including Ox Frame volcanics (Jr, and Ja), Harris Ranch Monzonite (Jh), Ruby Star megacrystic monzogranite (Tgx), and fine-grained diorite (TKd). The unit is apparently associated with emplacement of the megacrystic phase of the Ruby Star Granodiorite (Tgx). The Serrita Breccia of the pre-mine map was mapped as the andesite porphyry by Lynch (1967) who described the unit as a porphyritic, mafic intrusive unit that contained approximately 30% phenocrysts mostly of plagioclase but with significant amounts of hornblende and/or biotite. The phenocrysts were suspended in a finely crystalline matrix characterized by chloritic alteration and pervasive copper mineralization. According to Lynch (1967), the andesite porphyry was the most favorable host for supergene ore (some chalcocite zones assayed as high as 4% Cu) in the hills and peaks that have since been removed by mining. Lynch (1967) noted that during initial mining operations, oxide minerals gave way to chalcopyrite, pyrite, and molybdenite with increasing depth. Later, West and Aiken (1982) noted that as mining continued mineralization in the Sierrita Breccia decreased with depth.

Tmz Quartz monzonite dikes (Tertiary) – Fine- to medium-grained leucocratic dikes typically with feldspar-porphyritic texture (plagioclase 2-4mm and potassium feldspar 2-7mm), sparse quartz phenocrysts, and less than 5% altered mafic minerals. Composition probably ranges from quartz monzonite to monzonite. This unit correlates with the quartz latite porphyry of West and Aiken (1982). West and Aiken (1982) note that dikes in the pit area are mineralized with weak pyrite-chalcopyrite fracture coatings and fine-grained, disseminated pyrite. Hermann (2001) reports a U-Pb zircon age of 60 Ma from a dike along the western margin of the Sierrita pit.

Trd Rhyodacite porphyry (Tertiary) – A series of porphyritic dikes and small stocks in the Sierrita-Esperanza mine area. West and Aiken (1982) describe the rhyodacite porphyry as containing approximately 20% phenocrysts of zoned plagioclase, and myrmekitic potassium feldspar megacrysts (Smith, 1975). The dark gray to gray-green matrix consists of <1mm grains of quartz, orthoclase, oligoclase and biotite (Lynch's, 1967 dacite porphyry).

Tgf Sierrita Granite, aplite phase (Tertiary) – Fine-grained to aplitic leucogranite, locally containing 1-5% round quartz phenocrysts (2-5 mm). Contacts with medium- to coarse-grained leucogranite, the main phase of the Sierrita Granite (Tg) are sharp to gradational. Where contacts are sharp, Tgf intrudes Tg.

Tgfs Sierrita Granite, aplite phase in the Sierrita pit (Tertiary) – A single small stock of aplite exposed on the southern wall of the Sierrita pit, and tentatively correlated with the aplite phase of the Sierrita Granite (Tgf) in other parts of the Sierrita Mountains.

Tg Sierrita Granite (Tertiary) – Leucocratic, medium- to coarse-grained, equigranular granite to syenogranite with 1-5% mafic minerals, principally biotite in fine-grained aggregates, variably altered. A fine-grained to aplitic leucogranite phase (Tgf) is commonly present along contacts with host rocks. Locally, this phase contains 1-5% round quartz phenocrysts (2-5 mm). Contacts between the medium- to coarse-grained (Tg) and the fine-grained leucogranite phase are sharp to gradational. Where contacts are sharp, the fine-grained phase intrudes the medium- to coarse-grained phase. A transitional phase, not mapped separately, is characterized by 10-30% medium- to coarse-grained quartz and feldspar phenocrysts in a fine- to medium-grained groundmass, and is common in a stock located 1 km northeast of Lobo Peak. The term Sierrita Granite was first introduced by Lacey (1959) in reference to all of the granitic rocks exposed west of the Pima and Twin Buttes mines. Cooper (1973) reassigned many of these rocks to other units and retained the name Sierrita Granite for a distinctive suite of leucocratic granite. Cooper (1973) assigned a Jurassic age to the unit based on a Rb/Sr 137.1 $\pm$ 14.0Ma date from a highly altered zone along the northern edge of this map area (Damon, 1966). However, since the Sierrita Granite clearly intrudes the Paleocene Ruby Star Granodiorite, we assign a Paleocene age to the granite. Two Paleocene dates, a Rb/Sr date of 67.5 $\pm$ 6.0Ma (Damon, 1965), and a K/Ar biotite date of 56.4 + 3.0Ma (Marvin et al., 1973) that had been considered to young are reported from the Sierrita Granite in a large stock at Samaniego Peak just to the north of the map area.

Tns North Sierrita Porphyry (Tertiary) – Stocks of fine- to medium-grained biotite monzogranite with phenocrysts of potassium feldspar up to 2cm long and 5-10% biotite intrude the Ruby Star and West Sierrita Porphyry (Tgx and Tws) on the north side of the Sierrita-Esperanza pit. Hermann (2001) reports a U-Pb zircon date of 60.5 $\pm$ 0.2Ma from a stock in the north wall of the Sierrita-Esperanza pit.

Tws West Sierrita Porphyry (Tertiary) – Light gray to pinkish gray porphyritic monzogranite with up to 50% phenocrysts mainly of plagioclase (2-7mm), with subordinate potassium feldspar megacrysts (1 to 3 cm), and sub-rounded quartz eyes. The matrix consists of 1-5mm plagioclase, 0.5-3mm potassium feldspar, quartz, and biotite. The West Sierrita Porphyry was described as the Ruby Star Quartz Monzonite Porphyry by West and Aiken (1982). This unit grades to the north into the Ruby Star Granodiorite map units (Tgd, and Tgx) of this report.

Tgx Ruby Star Granodiorite, megacrystic phase (Tertiary) – Megacrystic, medium- to coarse-grained monzogranite to granodiorite, with 5-25% potassium feldspar megacrysts 1-5 cm long and 10-15% medium-grained, euhedral biotite. The megacrystic phase has been called “quartz monzonite porphyry” at the Sierrita-

Esperanza mine (West and Aiken 1982). Hermann (2001) reports a U-Pb zircon date of 63.4 ± 0.3Ma from the northeast corner of this map area.

Tgd **Ruby Star Granodiorite** (Tertiary) – The Ruby Star Granodiorite (Cooper 1973) forms a large composite pluton that is exposed throughout the northern Sierrita Mountains. The most abundant rock type in the pluton is medium-grained, equigranular granodiorite (Tgd). A transitional medium- to coarse-grained phase with up to 2% potassium feldspar megacrysts (0-100m thick) occurring between the main (Tgd) and megacrystic phase (Tgx) was not mapped separately. A U-Pb zircon date of 64.3Ma ± 0.4Ma (Hermann, 2001) was obtained for this unit in the Ocotillo pit, just northeast of the map area. Various other K/Ar biotite dates of ~37, 42, 47, 50, 51, and 63Ma have been reported from areas to the north of this map area (See summary in Reynolds et al., 1986)

TKd **Fine-grained, biotite diorite** (Tertiary) – Fine-grained diorite, 1-2% quartz, 20-40% mafic minerals (biotite, hornblende, and opaque oxide; chlorite and epidote are present as alteration products). Forms stocks that intrude the Harris Ranch Monzonite and older volcanic and sedimentary rocks. Marvin et al. (1973) obtained a K-Ar biotite date of 68.5 ± 2.0 Ma (recalculated by Shafiqullah and Langlois 1978 using modern decay constants) from the diorite 1 km west of the Sierrita-Esperanza mine. Although much of the diorite in the area appears fresh, the effects of hydrothermal alteration on the K-Ar systematics at the sample locality are unkown and, as such, this date may not be the age of the rock.

TKq **Quartz vein and hydrothermal breccia** (Tertiary – Cretaceous) – Zones of intense quartz vein intrusion, alteration, pervasive silicification, and brecciation of host rock. In many areas silicification appears to overprint zones of argillic alteration.

Cretaceous

Demetrie Andesite, eastern units

Ki Demetrie volcanics, intermediate porphyry (Cretaceous) – Aphanitic matrix, 15% plagioclase-porphyritic (1-3mm) porphyry containing sparse biotite phenocrysts. Occurs as a single small stock south of McGee Well in the northeast part of the map area.

Kdi Demetrie volcanics, intrusive andesite (Cretaceous) – Fine-grained crystalline to aphanitic matrix, plagioclase-porphyritic (5-15%, 1-2mm) andesite with sparse altered mafic phenocrysts. The stock occurs south of Horse Pasture Hill where it intrudes a south-dipping sequence of Red Boy Rhyolite (Jb). The stock is thought to be a feeder for extensive andesitic lava flows of the Demetrie Andesite exposed farther to the east.

Kd Demetrie volcanics, andesitic lava (Cretaceous) – Porphyritic andesitic to intermediate lava flows and possible hypabyssal equivalents. The lavas contain 5-40% 1-4mm subhedral to euhedral plagioclase phenocrysts, 2-15% <2mm altered mafic minerals. Some flows contain probable pyroxene phenocrysts and others contain pyroxene and biotite. The lavas occur in south-dipping, amalgamated sequence with rare mafic volcaniclastic sedimentary interbeds and three interbedded felsic pyroclastic units, two near the top of the succession exposed in this map area (Kdr and Kdw), and another much thicker unit near the base in the easterly adjacent map area (Kdlr of Spencer et al., 2003). The unit is at least 1.5km in total thickness and is everywhere overlain with angular unconformity by Tertiary conglomerate or volcanic rocks (Tcv or Ta). The composite unit is up to 1,000m thick.

Kdr Demetrie volcanics, upper rhyolite tuff (Cretaceous) – Light gray, welded rhyolite ash-flow tuff containing ~15% phenocrysts of anhedral quartz (<2mm, 7-10%), and strongly altered euhedral to subhedral feldspar (<1.5mm, 5-10%). Most of the feldspar phenocrysts appear to be altered plagioclase. The tuff contains little or no mafic minerals, and sparse lithic fragments (0-50m thick).

Kdw Demetrie volcanics, pyroclastic unit (Cretaceous) – A light colored, thin- to medium-bedded nonwelded pyroclastic and/or felsic volcaniclastic unit that locally includes clast-supported, phenocryst-poor rhyolite lava lapilli tuff breccia lenses (0-6m thick).

Kss Sandstone (Cretaceous) – Green-gray argillaceous, medium-grained feldspathic quartz sandstone. The unit is very poorly exposed, highly fractured, and tentatively correlated with the Angelica Arkose of Cooper (1973).

Jurassic

Jh Harris Ranch Monzonite (Jurassic) – Quartz monzonite, medium-grained, equigranular, greenish to pinkish gray, weathered light brown, containing 5-15% altered mafic minerals (epidotized amphibole?). Coarse-grained and fine-grained variations in texture occur within the main pluton. A fine-grained porphyritic variety, common near intrusive contacts and in dikes, contains 15-40% plagioclase phenocrysts (pink to light orange, subhedral to euhedral, 1-5mm) and up to 15% mafic minerals in a fine-grained to aphanitic, light pinkish gray to light green groundmass. Marvin et al. (1973) report a pair of problematic Pb-alpha dates for the Harris Ranch Monzonite of 190 $\pm$ 20Ma and 200 $\pm$ 30Ma from samples collected in the northern part of this map area (where the unit is strongly altered), and in the westerly adjacent Palo Alto

quadrangle. Marvin et al. (1973) also report a biotite K/Ar cooling age of 41.0 ± 2.0Ma from the sample to the west. Riggs et al. (1994) report an unpublished, concordant U-Pb zircon age of 177Ma for the Harris Ranch Monzonite, apparently collected somewhere in the Sierrita Mountains, but no location for this sample is known. Analytical data for the Riggs et al. (1994) date are included in Spencer et al. (in preparation).

Jhm Harris Ranch Monzonite, mafic phase (Jurassic) – Light gray, fine-grained, porphyritic monzonite to monzodiorite with up to 20% plagioclase phenocrysts (2-8mm) and 15-35% mafic minerals (hornblende and fine-grained biotite, altered to epidote and chlorite?). The mafic phase intrudes the Tascuela Canyon phase (Jht), but its contact with the main phase (Jh) appears to be gradational.

Jht Harris Ranch Monzonite, Tascuela Canyon phase (Jurassic) – Monzonite porphyry with medium-grained phenocrysts of potassium feldspar and plagioclase in a fine-grained to aphanitic, orange-pink groundmass.

Red Boy Rhyolite

Jbc Andesite-clast conglomerate, Red Boy Rhyolite (Jurassic) – Medium- to thick-bedded, mostly clast-supported, rounded to sub-rounded andesite-clast (chiefly pebble-cobble) conglomerate with dark-colored sandy matrix. Based on an apparent depositional upper contact with Red Boy Rhyolite mapped along Proctor Wash, the conglomerate is interpreted as a lens within the uppermost portion of the Red Boy Rhyolite (0-15m thick).

Jbd Dacitic ash-flow tuff, Red Boy Rhyolite (Jurassic) – Pink weathering moderately welded dacitic ash-flow tuff containing approximately 20% phenocrysts of feldspar (2-4mm) with up to 1% biotite (1-3mm). Occurs as a lens less than 50m thick interbedded within the upper part of the Red Boy Rhyolite along Proctor Wash. Age relationship to a nearbly lens of andesite-clast conglomerate (Jbc) unknown. This lens is probably a slightly more mafic variety of the nearby biotite-rich, quartz-phyric lenses of Red Boy Rhyolite (Jbb). The lens is 5-15m thick.

Jbb Biotite-rich ash-flow tuff, Red Boy Rhyolite (Jurassic) – Welded rhyolite ash-flow tuff containing 20-30% phenocrysts of plagioclase (1-3mm), potassium feldspar (1-3mm), and quartz (1-4mm) in subequal proportions, with up to 1% 1-3mm biotite phenocrysts. The unit occurs as a series of elongate lenses, typically less than 75m thick, interleaved with very sparsely biotite-phyric to biotite-absent Red Boy Rhyolite (Jb) near the top of a very thick intracaldera sequence exposed near Proctor Wash. The biotite-rich ash-flow tuff underlies an andesite-clast conglomerate (Jbc) and may be related genetically to a nearby dacitic ash-flow tuff lens (Jbd). Lenses are less than 30m thick.

Jb Rhyolite ash-flow tuff, Red Boy Rhyolite (Jurassic) – Rhyolite ash-flow tuff containing between 15-30% phenocrysts of plagioclase (0.5-1.5mm), quartz (1-4mm), and potassium feldspar (1-3mm) in roughly subequal proportions. In some areas, the base of the unit is characterized by a phenocryst-poor zone (5-7% phenocrysts). In general, the phenocryst content tends to increase up-section and the ratio of plagioclase:potassium feldspar increases indicating a normal zonation. In addition, little or no biotite phenocrysts are present throughout except near the top of the section

where sparse biotite is present, and lenses of biotite-rich ash-flow tuff (Jbb) occur. All exposures of the Red Boy Rhyolite in the map area lie within or near its source caldera, and large areas of the map unit are divided in mesobreccia (Jbz) and megabreccia (Jbx) units depending on the size and concentration of lithic fragments. In some areas, individual blocks of megabreccia are recognized (Jrp-Jb, Jt-Jb, and Jr-Jb) and mapped separately, as are zones of monolithic megabreccia (Jbdx and Jbrx). Clasts in the rhyolite porphyry megabreccia unit (Jbdx), the most voluminous unit within the caldera fill, have a similar phenocryst assemblage to the Red Boy Rhyolite and these units are interpreted to be co-magmatic. Pumice fragments of Red Boy Rhyolite are commonly indistinguishable from lithic clasts of the rhyolite porphyry (up to 2,000m thick).

Jbz Mesobreccia, Red Boy Rhyolite (Jurassic) – Rhyolite ash-flow tuff containing greater than 25% lithic fragments less than 1m in diameter.

Jbx Megabreccia, Red Boy Rhyolite (Jurassic) – Rhyolite ash-flow tuff containing greater than 25% lithic fragments, some of which are greater than 1m in diameter. In most cases lithic fragments in megabreccia are much greater than 1m, and commonly much greater than 10m.

Jbdx Rhyolite porphyry megabreccia, Red Boy Rhyolite (Jurassic) – Zones of megabreccia dominated by clasts of quartz-phyric rhyolite porphyry (map unit Jbd).

Jbrx Rhyolite lava megabreccia, Red Boy Rhyolite (Jurassic) – Zones of megabreccia dominated by clasts of phenocryst-poor rhyolite (map units Jr, Jrl, and Jrb).

Jrp-Jb Megaclasts of rhyolite porphyry, Red Boy Rhyolite (Jurassic) – Discreet megabreccia blocks of the rhyolite porphyry (Jrp) map unit.

Jt-Jb Megaclasts of phenocryst-rich dacite tuff, Red Boy Rhyolite (Jurassic) – Discreet megabreccia blocks of the phenocryst-rich dacite (Jt) map unit.

Jr-Jb Megaclasts of rhyolite lava, Red Boy Rhyolite (Jurassic) – Discreet megabreccia blocks of the phenocryst-poor rhyolite (Jr, Jrl, or Jrb) map unit.

Jrpw Western rhyolite porphyry (Jurassic) – Dikes and small stocks of ~10-15% phenocryst rhyolite porphyry. The porphyry contains subequal amounts of quartz (2-4mm), potassium feldspar (1-2mm), and plagioclase (1-2mm), and sparse biotite phenocrysts (0.5mm). Very sparse grains of white mica (<0.3mm) are also present. The porphyry is similar in appearance to the rhyolite porphyry (Jrp) unit that occurs mostly as megaclasts within the Red Boy Rhyolite (Jb), but can be distinguished because it contains biotite and its matrix tends to be pinkish gray in color (the Jrp rhyolite porphyry does not contain biotite and is characteristically light gray in color). The western rhyolite porphyry intrudes all Jurassic units in the George Tank area along the western edge of the study area. A dike of the unit cuts across the basal contact of the Red Boy Rhyolite (Jb) just to the east of Tascuela Canyon. Dikes of the porphyry are common within the tuff of George Tank (Jg) and in one area it appears that megaclasts within the tuff of George Tank are composed of this distinctive unit. The western rhyolite porphyry (Jrpw) therefore displays a similar relationship to the tuff of George Tank as is seen between the rhyolite porphyry (Jrp) and the Red Boy Rhyolite (Jb).

Jriu Rhyolite lava dike (Jurassic) – A single east-west striking rhyolite dike containing approximately 2-5% feldspar phenocrysts that intrudes andesitic lava (Jau) north of Lobo Peak. The dike is differentiated from nearby, petrographically similar, Ox Frame rhyolite dikes (Jr) based solely on the fact that it intrudes a sequence of andesite lava (Jau) interpreted to younger than Ox Frame andesite (Ja). The dike may be a feeder for the Jru rhyolite lava unit.

Jrp Rhyolite porphyry (Jurassic) – Moderately phenocryst-rich, flow-foliated rhyolite porphyry containing 20-30% phenocrysts of quartz (2-6mm), and feldspar (1-3mm). The unit occurs mostly as megaclasts within the Red Boy Rhyolite. The megaclasts commonly display brecciated textures reminiscent of lava autobreccia, and in some areas display sharp interdigitated, apparently intrusive contacts with the host Red Boy Rhyolite ash-flow tuff. The rhyolite porphyry is interpreted as an extensive sequence of lava domes that were emplaced just prior to and possibly shortly after eruption of the Red Boy Rhyolite. The lava domes are interpreted to have been catastrophically disrupted during the eruption and formation of the ash-flow tuff caldera. Much of the lava dome material may have been fluid at the time of disruption and emplaced as magmatic blebs within the intracaldera ash-flow tuff.

Jqu Quartz sandstone (Jurassic) – Thin sequences (<15m thick) of cross-stratified, gray quartz sandstone that directly underlies Red Boy Rhyolite megabreccia (Jbx) at Horse Pasture Peak. The sandstone is identical to units in the underlying Ox Frame volcanics (Jq) and is differentiated from these based solely on it its position above the angular unconformity that separates the units (0-15m thick).

Jru Rhyolite lava (Jurassic) – Rhyolite lava and rhyolite lava breccia containing approximately 5% phenocrysts of feldspar. The lava is identified in only one area, along the southern edge of the Sierrita Mountains near Horse Tank in SW/4 of Section 23, T18S, R11E. The lava is interpreted to be part of a south-southeast dipping sequence of volcanic rocks that unconformably overlies a complex area of hypabyssal Ox Frame andesite and rhyolite (Ja, Jr).

Jt Dacitic tuff (Jurassic) – Dark gray to purple phenocryst-rich dacitic ash-flow tuff containing up to 55% 1-2mm euhedral to subhedral plagioclase phenocrysts and 1-3% biotite. The tuff is welded in most areas, and exhibits a well-developed eutaxitic foliation. The tuff also contains up to 15% mafic volcanic lithic fragments similar to those found in the northerly adjacent andesitic conglomerate unit (Jc). The unit is interpreted to overlie the andesitic conglomerate (Jc), but the contact is not exposed (up to 200m thick).

Jtt Rhyodacite tuff (Jurassic) – Moderately phenocryst-rich rhyodacite ash-flow tuff containing ~10% 1-3mm, euhedral to subhedral plagioclase, ~5-7% 0.5-1.5mm, subhedral to anhedral quartz, ~2-5% 1-4mm subhedral to euhedral potassium feldspar, 1% 1mm biotite, and sparse <0.5mm opaque minerals. The unit occurs below the base of the Red Boy Rhyolite along the western edge of the map area. Age relationships with other Jurassic pre-caldera units unkown (~50m thick).

Jc Andesitic conglomerate (Jurassic) – A unit dominated by mafic volcaniclastic conglomerate interbedded with andesitic lava flows that is considered a western equivalent of a similar unit dominated by lava flows (Jau), exposed within the wall of

the Red Boy Peak caldera a few kilometers to the east. Lava flows make up less than 30% of this unit and consist of massive to autobrecciated plagioclase-porphyritic andesite. Hyaloclastite textures are preserved in some of the flows. Volcaniclastic rocks consist of massive to very thick-bedded and thick-bedded, matrix-supported and clast-supported andesite-clast conglomerate and conglomeratic sandstone. Sandy matrix is typically feldspathic and dark gray to purple in color. Clasts are dominated by andesite lava identical to the interbedded lava flows. Locally the conglomerate contains sparse clasts of intermediate volcanics, rare pink granitic rocks, and various sandstone-shale clasts. Clasts of the southerly adjacent dactitic ash-flow tuff (Jt) are not present. Along the northeast edge of its outcrop area, the unit contains conspicuous boulders of phenocryst-poor rhyolite lava derived from megaclasts within the adjacent tuff of George Tank (Jg). This relationship indicates that the unit is younger than the tuff of George Tank, but the nature of the contact is poorly understood. The contact is interpreted as a southwest-facing buttress unconformity that overlaps a southwest-side-down normal fault (up to 200m thick).

Jau Andesitic lava and conglomerate (Jurassic) – A unit dominated by andesitic lava flows that is considered an eastern equivalent of a similar unit dominated by andesitic conglomerate (Jc), exposed below the floor of the Red Boy Peak caldera a few kilometers to the west. Lava flows make up more than 70% of this unit and consist of massive to autobrecciated plagioclase-porphyritic andesite. Hyaloclastite textures are preserved in some of the flows. Volcaniclastic rocks consist of massive to very thick-bedded and thick-bedded, matrix-supported and clast-supported andesite-clast conglomerate and conglomeratic sandstone. Sandy matrix is typically feldspathic and dark gray to purple in color. Clasts are dominated by andesite lava identical to the interbedded lava flows. Locally the conglomerate contains sparse clasts of intermediate volcanics, rare pink granitic rocks, and various sandstone-shale clasts (probably > 300m thick).

Ox Frame volcanics (Jurassic?)

Jg Tuff of George Tank (Jurassic) – Megabreccia with matrix of moderately phenocryst-rich rhyolite ash-flow tuff containing 5-17% phenocrysts of anhedral quartz (1-8%, 0.5-2.5mm), euhedral to subhedral plagioclase (3-12%, 1-4mm), subhedral to euhedral potassium feldspar (<1-5%, 0.5-2mm), and sparse biotite (0.5-1mm). Although up to 2.5mm, quartz phenocrysts are rarely >1mm and characteristically rounded and anhedral in form. Both feldspars are intensely altered, and biotite, although sparse is present throughout the tuff, a diagnostic feature distinguishing this unit from the overlying Red Boy Rhyolite (Jb). The tuff of George Tank is found only along the western edge of the map area between Blackhawk Mine and George Tank and is almost entirely a megabreccia, containing 30-60% 1-100m blocks of rhyolitic and andesitic lava. Only the northwestern exposures of the unit contain less than 30% lithic fragments. Particularly large clasts of the northerly adjacent andesite lava map unit (Ja) occur in the megabreccia along its northern contact indicating that it is as a south-facing buttress unconformity. This unconformity is interpreted as a south-facing caldera margin or a syn-volcanic promontory (>300m thick).

Jr Rhyolite, undifferentiated (Jurassic) – Phenocryst-poor to aphyric rhyolite containing 0-5% phenocrysts of feldspar (1-2mm), sparse mafics and very rare quartz phenocrysts. Matrix is typically light gray, fine-grained and recrystallized. The rhyolite of this map unit is typically massive to flow-foliated.

Jrl Rhyolite lava (Jurassic) – Phenocryst-poor to aphyric rhyolite lava containing 0-5% phenocrysts of feldspar (1-2mm), sparse mafics and very rare quartz phenocrysts. Matrix is typically light gray, fine-grained and recrystallized. The rhyolite of this map unit shows evidence of volcanic textures, chiefly autobreccia, but large areas of the unit are also massive to flow-foliated coherent facies.

Jrb Rhyolite lava breccia (Jurassic) – Phenocryst-poor to aphyric rhyolite lava breccia containing 0-5% phenocrysts of feldspar (1-2mm), sparse mafics and very rare quartz phenocrysts. Matrix is typically light gray, fine-grained and recrystallized. Matrix of the autobreccia contains significant amounts of quartz sand at the top of many of the rhyolite lava flows in the Ox Frame Group. This unit is shown in areas where rhyolite autobreccia forms significantly large areas. In some areas these breccias may grade into clast-supported block and ash-flows.

Jrt Rhyolite tuff (Jurassic) – A single, phenocryst-poor, thin- to medium-bedded lens of nonwelded tuff mapped within a rhyolite lava sequence at Horse Pasture Hill (0-2m thick).

Jtq Rhyolite ash-flow tuff (Jurassic) – Moderately phenocryst-rich rhyolite ash-flow tuff containing 20-30% phenocrysts of quartz (0.5-2mm), plagioclase (0.5-2mm), and potassium feldspar (1-2mm) in roughly subequal amounts plus sparse biotite phenocrysts (<1mm). The tuff occurs as two discrete outflow sheets interbedded between rhyolitic and andesitic lava flows east of Ox Frame Canyon. (2-20m thick).

Jq Quartz sandstone (Jurassic) – Medium- to coarse-grained gray quartz sandstone that contains between 0-30% rhyolitic detrital clasts ranging in size from granules to pebbles. The rhyolitic clasts are commonly light colored and chalky in appearance, and the larger clasts are typically sub-angular to angular. Quartz sand is typically rounded and moderately well-sorted. The quartz sandstone unit occurs interbedded between andesitic and rhyolite lava flows throughout the Ox Frame Group (0-200m thick).

Jai Intrusive andesite (Jurassic) – A suite of dark colored andesitic rocks with fine-grained crystalline matrix and containing between 5-30% phenocrysts of plagioclase (1-6mm), and 0-5% strongly altered mafic minerals (generally <2mm). Map unit is shown in areas where intrusive nature is known.

Ja Andesite, undifferentiated (Jurassic) – A suite of dark colored andesitic rocks with fine-grained crystalline matrix and containing between 5-30% phenocrysts of plagioclase (1-6mm), and 0-5% strongly altered mafic minerals (generally <2mm).

Jal Andesite lava (Jurassic) – A suite of dark colored andesitic rocks with fine-grained crystalline matrix and containing between 5-30% phenocrysts of plagioclase (1-6mm), and 0-5% strongly altered mafic minerals (generally <2mm). Map unit shown in areas where volcanic origin is known based on contact relationships and volcanic textures, chiefly autobreccia. Most flows contain 10-15% euhedral to subhedral plagioclase phenocrysts (1-2mm), but some distinctive units are coarse-grained (3-6mm) and relatively phenocryst-rich (20-30%).

Jsj Tuff of San Juan Wash (Jurassic) – A pink, phenocryst-poor to aphyric rhyolite ash-flow tuff that contains sparse pumice and lithic fragments (0-5%).

Jsx Tuff of San Juan Wash megabreccia (Jurassic) – Zones of monolithic megabreccia within the tuff of San Juan Wash containing clasts (1-100m) of pink and red thin- to medium-bedded quartz sandstone, siltstone and mudstone. The zones of megabreccia typically contain up to and greater than 50% lithic blocks.

Paleozoic

PPh Horquilla Limestone (Pennsylvanian) – Strongly recrystallized cherty limestone epidote skarn and marble. Tentatively identified as Horquilla Limestone based on alternating bands of marble and epidote skarn interpreted as a metamorphosed sequence of medium-bedded limestone and siltstone-shale. Exposures just to the west of the map area include a weakly metamorphosed medium-bedded limestone-siltstone sequence dipping and facing to the south (>100m thick).

Me Escabrosa Limestone (Mississippian) – Strongly recrystallized massive limestone, locally cherty. Tentatively identified as Escabrosa Limestone based on stratigraphic position below the Horquilla Limestone (PPh), and massive appearance (~150m thick).

Proterozoic

Yg Granite (Mesoproterozoic) – Pink, medium- to coarse-grained, locally potassium feldspar porphyritic leucogranite containing less than 5% biotite.

Y-P$_z$-M$_z$* Pre-Tertiary rocks (Mesoproterozoic – Paleozoic – Mesozoic) – Undifferentiated granitic, volcanic, and sedimentary rocks.